Available online at www.sciencedirect.com

ScienceDirect

IFAC Papers Online CONFERENCE PAPER ARCHIVE

IFAC-PapersOnLine 48-1 (2015) 023–028

A compact mathematical model of mandelate racemase production and chaperone overexpression in *E. coli* ⋆

Bernhard Kramer * **Ralf Tüngler** * **Katja Bettenbrock** * **Carsten Conradi** *

* *Max Planck Institute for Dynamics of Complex Technical Systems, Sandtorstr. 1, 39106 Magdeburg, Germany (e-mail: kramer@mpi-magdeburg.mpg.de).*

Abstract: *E. coli* is commonly used for recombinant protein production, e.g. in the pharmaceutical industry for large-scale production of human insulin. A common problem arises from the formation of (often toxic) protein aggregates. The large number of process parameters complicates finding counter strategies by an empirical trial and error process. More promising seems the application of optimal control strategies based on mathematical modelling of target protein, heat shock proteins, and cell metabolism. However, by now no adequate mathematical model exists. As a first step we propose a small model that comprises the key players of recombinant protein formation, folding, aggregation/disaggregation, and degradation of the target protein mandelate racemase in *E. coli*. The model also includes the controlled overexpression of selected heat shock proteins (to date the native chaperone systems HSP70 and HSP60 in *E. coli*). Recombinant production of racemase and overexpression of chaperone systems is initiated by three different induction systems, one for each process. Hence the system has three input signals that later on can be used for control purposes. The model has been parametrised and fitted to appropriate experiments. Despite its limited size, the model explains biomass and chaperone production very well, while racemase production is not (yet) fully covered.

Keywords: Biotechnology, Mathematical modelling, Inclusion Bodies, Protein aggregation.

1. INTRODUCTION

E. coli is commonly used for recombinant protein synthesis (Schmidt *et al.*, 1999), e.g. in pharmaceutical industry for large-scale production of heterologous proteins like human insulin or other hormones (Carneiro *et al.*, 2013) as well as cytokines and many more (Ferrer-Miralles *et al.*, 2009).

The usually applied high target-protein (TP) expression rates cause profound changes in the cell metabolism (CM). Besides the high burden for the CM, which results in decreased growth rates and productivity (Carneiro *et al.*, 2013), the cells may also seriously suffer from toxicity of aggregates of the TP, commonly referred to as inclusion bodies (IBs). In addition conformational stress negatively influences the amount of soluble recombinant protein in the cell. Usually the stress-response machinery of the cells attempts to overcome this disadvantage by production of heat shock proteins (HSPs) like chaperones and proteases. The HSPs influence the correct folding and degradation of the TP and hence decrease the fraction of aggregates and therefore toxic effects (Hoffmann & Rinas, 2004a). Thereby productivity of active TP production is increased. But at the same time the stress-response implies further redirection of metabolic resources away from cell growth and TP production alone by stressing the CM due to increased synthesis of HSPs. Therefore it is important to find an optimal balance between TP and HSP production (Hoffmann & Rinas, 2004b).

In most cases the soluble recombinant TP conformation is desired (Villaverde & Carrió, 2003). A common method in industry is to go for high amounts of IBs which have to be purified after cultivation and cell harvesting. This causes additional challenges and costs after the cultivation process, as solubilization of IBs often requires hazardous chemicals.

A different approach to increase the amount of soluble recombinant TP is the in-situ concerted overexpression of chaperones (Kondo *et al.*, 2000; de Marco *et al.*, 2007; Haacke *et al.*, 2009; Nishihara *et al.*, 1998, 2000). Due to the complexity and specificity of the interaction between the TP and different chaperones the prediction of suitable expression strategies is not straight forward. Moreover various process parameters like growth temperature, media composition, inducer concentration, induction time, and plasmid-related properties like promotor strength and plasmid copy number affect protein biosynthesis (Miao & Kompala, 1992). Thus it is not conceivable to find optimal process conditions by an empiric trial and error approach (Villaverde & Carrió, 2003). More promising methods aim at utilising optimal control concepts based on mathematical models. However by now no adequate mathematical model exists that describes the complex dynamic behaviour of recombinant protein synthesis, IB

⋆ BK & CC acknowledge funding by the research focus dynamical systems of the state Saxony-Anhalt.

10.1016/j.ifacol.2015.05.075

formation, interaction with HSPs, and the influence on the CM (Carneiro *et al.*, 2013).

Here we propose a compact mathematical model describing the recombinant formation, folding, aggregation/disaggregation, and degradation of the TP mandelate racemase (MR) for certain process parameters including the influence of selected HSPs. We parametrise and validate our model based on experimental data. The recombinant production of MR in *E. coli* serves as a model system. MR catalyses the racemisation of mandelate, also denoted as mandelic acid (MA), and its derivatives. MA and its derivatives are eminent educts for the production of several active pharmaceutical ingredients in pharmaceutical industry (Xu & Chen, 2008; Wang *et al.*, 2012).

As a basis for the mathematical modelling, biological background knowledge of the TP, several chaperones and proteases and their interaction is summarised in section 2. The mathematical model is then described in section 3, the parametrisation of the model follows in section 4. Finally, in section 5, results and conclusions are discussed.

2. BIOLOGICAL BACKGROUND

2.1 E. coli

E. coli is a Gram-negative, rod-shaped bacterium of the family of *Enterobacteriaceae* (Brenner *et al.*, 2005). Under optimal growth conditions its replication time is about 20 min (Neidhardt, 1996). Since the first complete DNA sequence mapping in 1997 it has become more and more important in biotechnological engineering and industrial microbiology and it has been established as an important host for the production of heterologous proteins. Easy availability and cultivation without particular danger as well as the comparatively simple plasmid transformation and protein-labeling also make *E. coli* an important model organism in research (Neidhardt, 1996). The strain *E. coli* BL21(DE3) is frequently used for the expression of recombinant DNA applying different promotors (Daegelen *et al.*, 2009), especially the T7-RNA-polymerase controlled promotor.

2.2 Mandelate & Mandelate Racemase

MA, also called α-hydroxy phenylacetic acid, is an aromatic organic acid and an important educt for the production of active pharmaceutical ingredients (e.g. for production of antibiotics or medicaments in cancer therapy (Xu & Chen, 2008)). Some microorganisms use MA as carbon and energy source. It appears as enantiomer, that is, in two steric conformations. This phenomenon is called chirality. The microorganism *Pseudomonas putida*, for example, can metabolise the (S)-enantiomer of MA, but not the (R)-enantiomer. This is converted to the (S)-conformation by MR (Tsou *et al.*, 1990).

MR (EC 5.1.2.2) is an enzyme of the group of racemases and was first isolated from *Pseudomonas putida* (Stecher *et al.*, 1998). The activity of MR does not rely on cofactors (Stecher *et al.*, 1998) but on divalent metal ions, with Mg^{2+} achieving the fastest conversion (Fee *et al.*, 1974). Besides the natural substrate MA, different p-substituted MA-derivatives and substances structurally less based on MA can be converted by MR (Stecher *et al.*, 1998).

2.3 Chaperones, Proteases & the Heat Shock Answer

Newly synthesised proteins usually reach their native, relatively stable conformation on their own. However 10 - 20 % of proteins need assistance by chaperones. Chaperones prevent aggregation during protein folding and unfolding, influence yield and kinetics of the folding, and have effects in regions of stoichiometric concentrations (Jakob & Buchner, 1994). They are an essential part of the cell and can be found in procaryotes as well as eucaryotes (Hoffmann & Rinas, 2004a).

Proteins are degraded by proteases if the folding fails or if errors during transcription or translation occur. This happens for around 20 % of newly synthesised proteins. Chaperones and proteases detect denatured polypeptides by exposed hydrophobe regions, which in native conformation are hidden in the molecule's interior. For a detailed description of the interplay of chaperones and proteases during the folding process see Gottesman *et al.* (1997); Wickner (1999).

Proteins which do not take their native conformation or get degraded, aggregate to form IBs, porous, egg-shaped or cylindrical structures of high density. IBs are a direct consequence of a survival strategy in stress situations. Under physiological conditions their presence is not reasonable, because they reduce the amount of available amino acids, interfere cellular functions, and may induce aggregation of other proteins (Wickner, 1999). The single polypeptides of the IBs can be transformed into the native conformation or degraded by the proteins of the heat shock answer (HSA) (Villaverde & Carrió, 2003).

High temperatures and other stress situations like osmotic shocks, dehydration or mutations can denature and subsequently aggregate proteins (Ben-Zvi & Goloubinoff, 2001). The cell tries to prevent this by the HSA, leading to increased expression of HSPs like chaperones and proteases (Hoffmann & Rinas, 2004a). The ATP-dependant folding of a denatured protein is energetically favourable to the new synthesis of the polypetide (Bukau & Horwich, 1998).

Here we focus on the HSP70- and HSP60-families, and on proteases. DnaK is the central molecule of the HSP70-family with its co-chaperones DnaJ and GrpE (Bukau & Horwich, 1998), together referred to as KJE system. KJE is essential for the cell (Hoffmann & Rinas, 2004a) as it disaggregates IBs to unfolded proteins. In *E. coli* GroEL is the HSP60 which forms a functional unit together with its co-chaperone GroES (Hoffmann & Rinas, 2004a), together referred to as ELS system. ELS represents an essential folding assistant as it intensifies the formation of native protein conformations from unfolded protein. Both, KJE and ELS work ATP-dependant. For a detailed summary, also including additional chaperone systems see Gross (1996); Hoffmann & Rinas (2004a).

3. MATHEMATICAL MODEL

During the recombinant production of MR in *E. coli* different protein conformations occur, from unfolded polypeptide chains to native TP. Enzymatic activity is expected

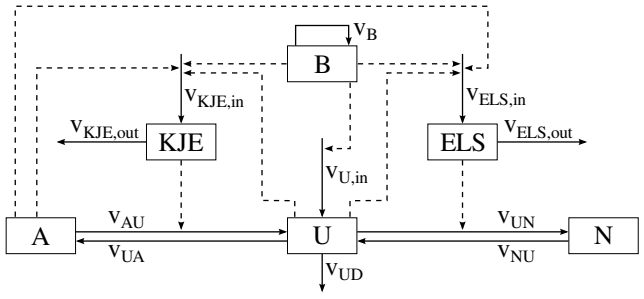

Fig. 1. Graph of ODE model of MR species interaction, chaperone species influence, and B formation. Solid arrows denote reaction rates v, dashed arrows influence of species as modifiers. Production of unfolded and dissolved MR species U ($v_{U,in}$) and chaperones KJE and ELS ($v_{KJE,in}, v_{ELS,in}$) is dependant on B, which is formed proportional to itself (v_B). U may reach the native conformation N of MR catalysed by ELS (v_{UN}), which in turn may denature to U without ELS influence (v_{NU}). U forms aggregates A of MR (v_{UA}), which in turn disaggregate to U catalysed by KJE (v_{AU}). Both A and U act as modifiers, inducing production of KJE and ELS. U may degrade (v_{UD}), as well as KJE and ELS may degrade ($v_{KJE,out}, v_{ELS,out}$).

only in native TP, although non native conformation may show biological activity (García-Fruitós *et al.*, 2007; Martínez-Alonso *et al.*, 2007). Preliminary experiments with recombinant MR production showed IB formation (data not shown). Therefore MR needs folding assistance by several chaperone systems.

We consider the cell as an ideally mixed chemical reactor, with enzyme-catalysed reactions and without substrate limitation. Hence energy species (ATP, ADP, redox equivalents) conversion and impact on metabolism is neglected. Our model consists of six species: Biomass B (considered equivalent to the optical density), MR conformations A (aggregates, representing IBs), U (unfolded, dissolved), N (native, dissolved), and chaperone systems KJE and ELS. B is defined to be dimensionless. All other species are expressed in the unit mg/L. The functional relations between MR conformations and chaperones are illustrated in Fig. 1. The corresponding ordinary differential equations (ODEs) describe B formation, B-dependant formation of MR, MR degradation, chaperone-assisted conversion of MR conformations, and chaperone formation and degradation:

$$\dot{x}_B = v_B \tag{1}$$
$$\dot{x}_{KJE} = v_{KJE,in} - v_{KJE,out} \tag{2}$$
$$\dot{x}_{ELS} = v_{ELS,in} - v_{ELS,out} \tag{3}$$
$$\dot{x}_U = v_{U,in} - v_{UN} + v_{NU} - v_{UD} - v_{UA} + v_{AU} \tag{4}$$
$$\dot{x}_N = v_{UN} - v_{NU} \tag{5}$$
$$\dot{x}_A = v_{UA} - v_{AU}. \tag{6}$$

The rates v_i are explained in the following: B formation v_B in (7) is assumed to be proportional to B concentration x_B:

$$v_B = \mu_{eff}\, x_B, \tag{7}$$

where μ_{eff} is the effective growth rate given below. The effective growth rate μ_{eff} summarises the following effects: Heterologous protein production stresses CM and hence reduces B formation. Heterologous production of MR is induced by isopropyl β-D-1-thiogalactopyranoside (IPTG), production of KJE is induced by arabinose (Ara) and production of ELS by anhydrotetracycline (Tet). Biosynthesis can be inhibited by addition of spectinomycin (Spec). To incorporate these effects in μ_{eff}, we use variables x_{IPTG}, x_{Ara}, x_{Tet}, and x_{Spec} to denote inducer and spectinomycin concentrations as well as prameters μ_{max} (maximal growth rate) and $\mu_{IPTG,inh}$, $\mu_{Ara,inh}$, $\mu_{Tet,inh}$ (inhibiting inducer effects):

$$\mu_{eff} = (1 - x_{Spec}) \cdot \big(\mu_{max} - \mu_{IPTG,inh} \cdot x_{IPTG} - \mu_{Ara,inh} \cdot x_{Ara} - \mu_{Tet,inh} \cdot x_{Tet}\big) \tag{8}$$

The variable x_{Spec} is either 0 or 1, corresponding to no inhibition and full inhibition, respectively. Note that cell death is neglected and therefore μ_{max} is defined as the difference between an absolute maximum growth rate and a cell decease rate, appearing as a relative growth rate.

Inhibition of biosynthesis by Spec is also considered in the production rates of chaperones and unfolded MR $v_{KJE,in}$, $_{ELS,in}$, and $v_{U,in}$ in (9), (10) & (11) below. Each of the rates consists of three terms, describing basal, stress-dependant, and inducer-dependant rates, respectively, where basal rates for the chaperones also describe native cellular expression.

$$v_{KJE,in} = (v_{KJE,basal} + v_{KJE,stress} + v_{KJE,ind}) \cdot (1 - x_{Spec}) \tag{9}$$
$$v_{ELS,in} = (v_{ELS,basal} + v_{ELS,stress} + v_{ELS,ind}) \cdot (1 - x_{Spec}) \tag{10}$$
$$v_{U,in} = (v_{U,basal} + v_{U,ind}) \cdot (1 - x_{Spec}) \tag{11}$$

Rates $v_{KJE,basal}$, $v_{ELS,basal}$, and $v_{U,basal}$ in (12), (13) & (14) are introduced to describe the leaky expression of the plasmids:

$$v_{KJE,basal} = k_{KJE,basal} \cdot x_B \tag{12}$$
$$v_{ELS,basal} = k_{ELS,basal} \cdot x_B \tag{13}$$
$$v_{U,basal} = k_{U,basal} \cdot x_B \tag{14}$$

Stress-dependant rates $v_{KJE,stress}$ and $v_{ELS,stress}$ in (15) & (16) describe the native stress response due to IB formation (initiated by unfolded x_U and aggregated x_A) and are formulated as a Michaelis-Menten like kinetic with x_B as substrate:

$$v_{KJE,stress} = \frac{k_{cat,KJE,AU,stress} \cdot (x_A + x_U) \cdot x_B}{K_{m,KJE,AU,stress} + x_B} \tag{15}$$
$$v_{ELS,stress} = \frac{k_{cat,ELS,AU,stress} \cdot (x_A + x_U) \cdot x_B}{K_{m,ELS,AU,stress} + x_B} \tag{16}$$

Inducer-dependant rates $v_{KJE,ind}$, $v_{ELS,ind}$, and $v_{U,ind}$ in (17), (18) & (19) are also formulated as a Michaelis-Menten like kinetic, depending on inducer concentration x_{Ara}, x_{Tet}, and x_{IPTG} and with x_B as substrate:

$$v_{KJE,ind} = \frac{k_{cat,KJE,Ara,ind} \cdot x_{Ara} \cdot x_B}{K_{m,KJE,Ara,ind} + x_B} \tag{17}$$
$$v_{ELS,ind} = \frac{k_{cat,ELS,Tet,ind} \cdot x_{Tet} \cdot x_B}{K_{m,ELS,Tet,ind} + x_B} \tag{18}$$
$$v_{U,ind} = \frac{k_{cat,U,IPTG,ind} \cdot x_{IPTG} \cdot x_B}{K_{m,U,IPTG,ind} + x_B} \tag{19}$$

Chaperone degradation rates $v_{KJE,out}$ & $v_{ELS,out}$ in (20) & (21) are formulated proportional to the respective chaperone concentration:

$$v_{KJE,out} = k_{KJE,out} \cdot x_{KJE} \tag{20}$$

$$v_{ELS,out} = k_{ELS,out} \cdot x_{ELS} \tag{21}$$

The MR species interconversion rates v_{NU} and v_{UA} in (22) & (23) and the degradation rate of unfolded MR v_{UD} in (24) are also formulated proportional to the species concentration:

$$v_{NU} = k_{NU} \cdot x_N \tag{22}$$
$$v_{UA} = k_{UA} \cdot x_U \tag{23}$$
$$v_{UD} = k_{UD} \cdot x_U \tag{24}$$

The ELS catalysed folding of U with rate v_{UN} in (25) is formulated as Michaelis Menten kinetics with x_U as substrate concentration and x_{ELS} as enzyme concentration:

$$v_{UN} = \frac{k_{cat,UN,ELS} \cdot x_{ELS} \cdot x_U}{K_{m,UN,ELS} + x_U} \tag{25}$$

The disaggregation rate of A to U v_{AU} in (26) is formulated as irreversible competitive product inhibition with x_A as substrate and x_U as competitive inhibiting product:

$$v_{AU} = \frac{k_{cat,AU,KJE} \cdot x_{KJE} \cdot x_A}{K_{m,A,KJE} \cdot \left(1 + \frac{x_U}{K_{m,U,KJE}}\right) + x_A} \tag{26}$$

In summary, the model comprises six state variables and ODEs, four input variables (the inducer and inhibitor concentrations), eleven primary rates, eight secondary rates, and twenty-seven parameters.

4. EXPERIMENTS

To fit our model parameters we use time series measurements of *E. coli* BL21(DE3) transformed with two plasmids. The plasmid for MR expression (Stephen L. Bearne, Department of Biochemistry and Molecular Biology, Dalhousie University, Halifax, NS, Canada B3H 1X5) is inducible by IPTG. The second plasmid (pG-KJE8 from TaKaRa (2013)) enables KJE induction by Ara and ELS induction by Tet. The main *E. coli* batch culture grows in shake flasks with minimal medium with glucose and trace elements, at 37°C and 250 rpm, and with appropriate antibiotics (ampicillin, chloramphenicol). An overnight grown inocolum is given to the main culture medium so that it starts with an optical density, always measured at 420 nm, of OD 0.1. We induce at OD 0.2 and stop biosynthesis via Spec before the exponential growth phase ends. Samples of culture liquid are taken at appropriate time points during growth, washed, and afterwards cells are disrupted via ultrasonification. This way we get, after centrifugation and washing steps, aggregates A in the pellet, and unfolded U as well as native N in solution. With SDS-PAGE we quantify the amounts of KJE, ELS, A, and the sum of U and N. Using laser polarimetry we measure the change in optical rotation during racemisation of MA enantiomers with added solution of U+N. We assume only the native active protein catalyses the racemisation of MA enantiomers and therefore this method enables us to quantify the amount of N in solution.

5. RESULTS & CONCLUSION

For modelling and fitting we use the Matlab toolbox PottersWheel 3.1.2 (Maiwald & Timmer, 2008). The toolbox is set to use Sundials CVODES integrator and the logarithmic trust region optimisation method with maximum 400 iterations per fit sequence for fitting. To fit the model

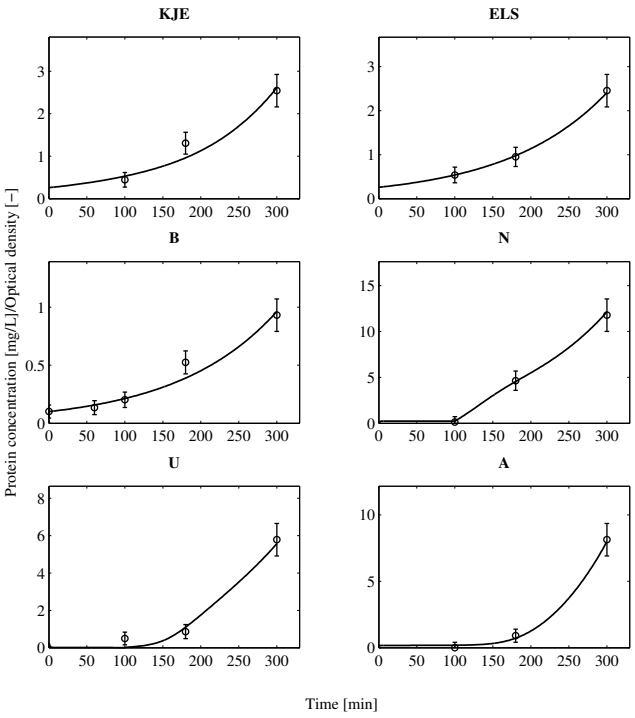

Fig. 2. Simulation results for scenario 1, induction of MR with IPTG at OD 0.2 (100 min). Unit for all species is mg/L, except for B it is dimensionless. Open circles denote measured values, solid lines simulation results. Error bars arise from PottersWheel error model as in (28).

function to the data points, an objective function $\chi^2(p)$ in (27) is minimised.

$$\chi^2(p) = \sum_{i=1}^{N} \left(\frac{y_{data}(i) - y_{model}(i,p)}{\sigma(i)} \right)^2 \tag{27}$$

Data point i is represented by $y_{data}(i)$, $\sigma(i)$ is the standard deviation w.r.t. N data points, and $y_{model}(i,p)$ is the model value corresponding to data point i and parameter set p. An optimal fit would result in $\chi^2/N \leq 1$. Two time series measurements of batch cultures as described in section 4 with differing induction scheme (scenarios) are fitted simultaneously. We consider the change in the input variables as step function, i.e. zero for no induction and one for induced. This is justified since we use the same inducer concentration in all experiments, if induction is applied.

In scenario 1, shown in Fig. 2 we induce MR expression via IPTG. As it is a single time series, no standard deviation of the measured data can be calculated. Therefore PottersWheel uses an error model with 10% relative and 5% absolute error for $\sigma(i)$ in (28).

$$\sigma(i) = 0,10 \cdot y_{data}(i) + 0,05 \cdot max(y_{data}) \tag{28}$$

Here $max(y_{data})$ is the maximum value of the time series. Biosynthesis is inhibited by Spec at 376 min. In scenario 2, shown in Fig. 3 we induce KJE and ELS parallel via Ara and Tet. Here the standard deviation is calculated from three biological replicates. Biosynthesis is inhibited by Spec at 640 min.

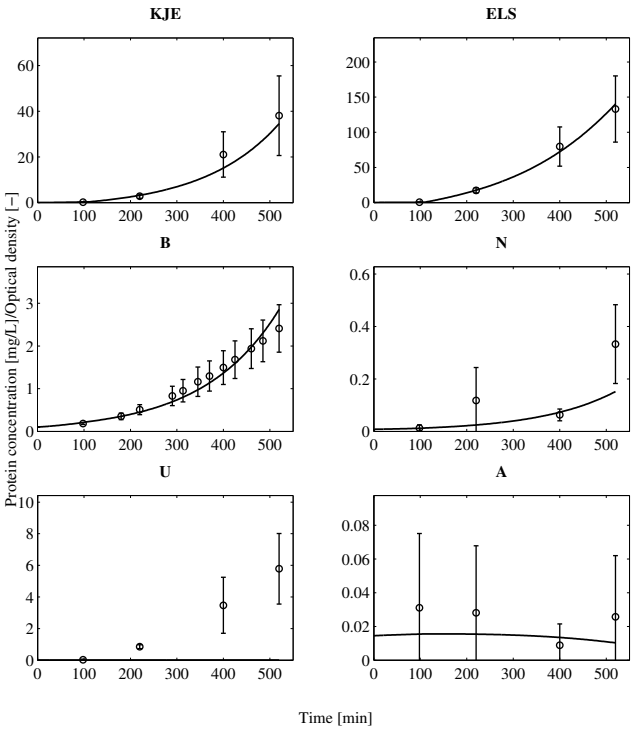

Fig. 3. Simulation results for scenario 2, induction of KJE and ELS with Ara and Tet at OD 0.2 (110 min). Unit for all species is mg/L, except for B it is dimensionless. Open circles denote measured values, solid lines simulation results. Error bars arise from standard deviation calculated from three biological replicates.

We use the in PottersWheel included F2 fit procedure with 500 fit sequences in a row (parameter disturbance strength 0.5) with parameters free between values of $1{\cdot}exp\,(-6)$ and $1{\cdot}exp\,(+4)$. We set the start values of the six state variables to 0.001 mg/L, except for B it is 0.1 (dimensionless). Every fit sequence in the F2 procedure starts with disturbed initial parameter values of the first fit. The best fit of the F2 procedure is used as starting point for a F3 fit procedure with 500 fit sequences in a row (parameter disturbance strength 0.2). There the parameters are free between the initial parameter values (parameter values of the best fit of the F2 sequence) divided by 1.3 and the initial parameter values multiplied with 1.3. Every fit sequence in the F3 procedure starts with disturbed parameters of the so far best fit of the F3 procedure. This way, considering the number of data points $N = 53$, the best overall fit quality of $\chi^2/N = 1.7$ is obtained. Please see table A.1 in the appendix A for information regarding parameter values.

For both scenarios x_B is able to explain the experimental data very well (cf. Figs. 2 & 3). Unfortunately, in scenario 2 the time course data of x_U cannot be explained, whereas the time course data of x_N, and x_A can be regarded as described good enough within their standard deviation (depicted by the error bars). However, in scenario 1 the time course data of these species can be explained sufficiently good. The chaperone species x_{KJE} and x_{ELS} can be explained sufficiently good in both scenarios.

In summary, the model is able to explain B formation and chaperone conversion, but fails to explain the MR species and their production and conversion in scenario 2. We believe that this is a consequence of our decision to neglect other chaperone systems in the model (in particular the trigger factor). Nonetheless we are confident that by including other chaperone systems our model will be able to explain all experimental data sufficiently well. Therefore we view the present model as an important first step in obatining a mathematical model of chaperone-assisted TP production that is suitable for process optimisation.

Implementation of possible control strategies based on the variation of the three input signals IPTG, Ara and Tet requires further work on the model structure and design of suitable experiments. In particular the three input-signal-linked input rates of B, KJE and ELS, i.e. v_B, $v_{KJE,ind}$ and $v_{ELS,ind}$, which are currently modelled as step functions, are adapted in future work. Rate formulations corresponding to sigmoid functions likewise the well known Hill kinetics are conceivable.

REFERENCES

S. Carneiro, E. C. Ferreira & I. Rocha (2013). Metabolic responses to recombinant bioprocesses in *Escherichia coli*. *Journal of Biotechnology 164*(3), 396–408.

M. Schmidt, E. Viaplana, F. Hoffmann, S. Marten, A. Villaverde & U. Rinas (1999). Secretion-dependent proteolysis of heterologous protein by recombinant *Escherichia coli* is connected to an increased activity of the energy-generating dissimilatory pathway. *Biotechnology and Bioengineering 66*(1), 61–67.

N. Ferrer-Miralles, J. Domingo-Espín, J. L. Corchero, E. Vázquez & A. Villaverde (2009). Microbial factories for recombinant pharmaceuticals. *Microbial Cell Factories 8*(17).

F. Hoffmann & U. Rinas (2004a). Roles of heat-shock chaperones in the production of recombinant proteins in *Escherichia coli*. In *Physiological stress responses in bioprocesses*, Volume 89 of *Advances in Biochemical Engineering*, pp. 143–161. Springer Berlin Heidelberg.

F. Hoffmann & U. Rinas (2004b). Stress induced by recombinant protein production in *Escherichia coli*. In *Physiological stress responses in bioprocesses*, Volume 89 of *Advances in Biochemical Engineering*, pp. 73–92. Springer Berlin Heidelberg.

A. Villaverde & M. M. Carrió (2003). Protein aggregation in recombinant bacteria: Biological role of inclusion bodies. *Biotechnology Letters 25*(17), 1385–1395.

A. Kondo, J. Kohda, Y. Endo, T. Shiromizu, Y. Kurokawa, K. Nishihara, H. Yanagi, T. Yura & H. Fukuda (2000). Improvement of productivity of active horseradish peroxidase in *Escherichia coli* by coexpression of Dsb proteins. *Journal of Bioscience and Bioengineering 90*(6), 600–606.

A. de Marco, E. Deuerling, A. Mogk, T. Tomoyasu & B. Bukau (2007). Chaperone-based procedure to increase yields of soluble recombinant proteins produced in *E. coli*. *BMC Biotechnology 7*(1), 32.

A. Haacke, G. Fendrich, P. Ramage & M. Geiser (2009). Chaperone over-expression in *Escherichia coli*: Apparent increased yields of soluble recombinant protein kinases are due mainly to soluble aggregates. *Protein Expression and Purification 64*(2), 185–193.

K. Nishihara, M. Kanemori, M. Kitagawa, H. Yanagi & T. Yura (1998). Chaperone coexpression plasmids: Differential and synergistic roles of DnaK-DnaJ-GrpE and GroEL-GroES in assisting folding of an allergen of Japanese cedar pollen, Cryj2, in *Escherichia coli*. *Applied and environmental microbiology 64*(5), 1694–1699.

K. Nishihara, M. Kanemori, H. Yanagi & T. Yura (2000). Overexpression of trigger factor prevents aggregation of recombinant proteins in *Escherichia coli*. *Applied and environmental microbiology 66*(3), 884–889.

F. Miao & D. S. Kompala (1992). Overexpression of cloned genes using recombinant *Escherichia coli* regulated by a T7 promoter: I. Batch cultures and kinetic modeling. *Biotechnology and Bioengineering 40*(7), 787–796.

H. Xu & Y. Chen (2008). An efficient and practical synthesis of mandelic acid by combination of complex phase transfer catalyst and ultrasonic irradiation. *Ultrasonics Sonochemistry 15*(6), 930–932.

P. Wang, E. Zhang, P. Zhao, Q.-H. Ren, Y.-Y. Guan & H.-M. Liu (2012). Diastereomeric resolution of racemic *o*-chloromandelic acid. *Chirality 24*(12), 1013–1017.

D. J. Brenner, N. R. Krieg & J. T. Staley (2005). *Bergey's manual of systematic bacteriology: The Proteobacteria* (2 ed.). New York: Springer.

F. C. Neidhardt (1996). The enteric bacterial cell and the age of bacteria. In F. C. Neidhardt (Ed.), *Escherichia coli and Salmonella typhimurium*, pp. 1–3. Washington and D.C: American Society for Microbiology.

P. Daegelen, F. W. Studier, R. E. Lenski, S. Cure & J. F. Kim (2009). Tracing ancestors and relatives of *Escherichia coli* B, and the derivation of B strains REL606 and BL21(DE3). *Journal of molecular biology 394*(4), 634–643.

F. Studier & B. A. Moffatt (1986). Use of bacteriophage T7 RNA polymerase to direct selective high-level expression of cloned genes. *Journal of Molecular Biology 189*(1), 113–130.

A. Y. Tsou, S. C. Ransom, J. A. Gerlt, D. D. Buechter, P. C. Babbitt & G. L. Kenyon (1990). Mandelate pathway of *Pseudomonas putida*: Sequence relationships involving mandelate racemase, (S)-mandelate dehydrogenase, and benzoylformate decarboxylase and expression of benzoylformate decarboxylase in *Escherichia coli*. *Biochemistry 29*(42), 9856–9862.

H. Stecher, A. Hermetter & K. Faber (1998). Mandelate racemase assayed by polarimetry. *Biotechnology Techniques 12*(3), 257–261.

J. A. Fee, G. D. Hegeman & G. L. Kenyon (1974). Mandelate racemase from *Pseudomonas putida*. Subunit composition and absolute divalent metal ion requirement. *Biochemistry 13*(12), 2528–2532.

U. Jakob & J. Buchner (1994). Assisting spontaneity: The role of Hsp90 and small Hsps as molecular chaperones. *Trends in Biochemical Sciences 19*(5), 205–211.

S. Gottesman, S. Wickner & M. R. Maurizi (1997). Protein quality control: Triage by chaperones and proteases. *Genes & development 11*(7), 815–823.

S. Wickner (1999). Posttranslational quality control: Folding, refolding, and degrading proteins. *Science 286*(5446), 1888–1893.

A. P. Ben-Zvi & P. Goloubinoff (2001). Review: Mechanisms of disaggregation and refolding of stable protein aggregates by molecular chaperones. *Journal of Structural Biology 135*(2), 84–93.

B. Bukau & A. L. Horwich (1998). The Hsp70 and Hsp60 Chaperone Machines. *Cell 92*(3), 351–366.

C. A. Gross (1996). Function and regulation of the heat shock proteins. In F. C. Neidhardt (Ed.), *Escherichia coli and Salmonella typhimurium*, pp. 1382–1399. Washington and D.C: American Society for Microbiology.

S. Gottesman (1996). Proteases and their targets in *Escherichia coli*. *Annual Review of Genetics 30*(1), 465–506.

E. García-Fruitós, M. Martínez-Alonso, N. Gonzàlez-Montalbán, M. Valli, D. Mattanovich & A. Villaverde (2007). Divergent genetic control of protein solubility and conformational quality in *Escherichia coli*. *Journal of Molecular Biology 374*(1), 195–205.

M. Martínez-Alonso, A. Vera & A. Villaverde (2007). Role of the chaperone DnaK in protein solubility and conformational quality in inclusion body-forming *Escherichia coli* cells. *FEMS Microbiology Letters 273*(2), 187–195.

TaKaRa (20.11.2013). Chaperone plasmid set user manual: `http://www.ibt.unam.mx/computo/cepas/manual_Chaperone_plasmid_set.pdf`.

T. Maiwald & J. Timmer (2008). Dynamical modeling and multi-experiment fitting with PottersWheel. *Bioinformatics 24*(18), 2037–2043.

Appendix A. PARAMETER VALUES

Table A.1. Initial and fitted parameter values

Parameter	Initial value	Fitted value	Unit
μ_{max}	$1 \cdot exp(-2)$	$7.546039 \cdot exp(-3)$	$1/min$
$\mu_{IPTG,inh}$	$1 \cdot exp(-3)$	$7.692442 \cdot exp(-7)$	$1/min$
$\mu_{Ara,inh}$	$1 \cdot exp(-3)$	$9.201967 \cdot exp(-4)$	$1/min$
$\mu_{Tet,inh}$	$1 \cdot exp(-3)$	$4.751655 \cdot exp(-4)$	$1/min$
$k_{KJE,basal}$	$1 \cdot exp(0)$	$1.760049 \cdot exp(-2)$	$mg/(L \cdot min)$
$k_{ELS,basal}$	$1 \cdot exp(0)$	$2.418210 \cdot exp(-2)$	$mg/(L \cdot min)$
$k_{U,basal}$	$1 \cdot exp(0)$	$3.129143 \cdot exp(-4)$	$mg/(L \cdot min)$
$k_{cat,KJE,AU,stress}$	$1 \cdot exp(+1)$	$3.848422 \cdot exp(-4)$	$1/min$
$K_{m,KJE,AU,stress}$	$1 \cdot exp(-2)$	$8.345696 \cdot exp(-7)$	-
$k_{cat,ELS,AU,stress}$	$1 \cdot exp(+1)$	$7.692327 \cdot exp(-7)$	$1/min$
$K_{m,ELS,AU,stress}$	$1 \cdot exp(-2)$	$1.300000 \cdot exp(+4)$	-
$k_{cat,KJE,Ara,ind}$	$1 \cdot exp(+1)$	$5.149398 \cdot exp(+2)$	$mg/(L \cdot min)$
$K_{m,KJE,Ara,ind}$	$1 \cdot exp(-2)$	$8.221423 \cdot exp(+3)$	-
$k_{cat,ELS,Tet,ind}$	$1 \cdot exp(+1)$	$2.312030 \cdot exp(0)$	$mg/(L \cdot min)$
$K_{m,ELS,Tet,ind}$	$1 \cdot exp(-2)$	$4.242506 \cdot exp(0)$	-
$k_{cat,U,IPTG,ind}$	$1 \cdot exp(+1)$	$1.286253 \cdot exp(+2)$	$mg/(L \cdot min)$
$K_{m,U,IPTG,ind}$	$1 \cdot exp(-2)$	$5.057698 \cdot exp(+2)$	-
$k_{KJE,out}$	$1 \cdot exp(-3)$	$7.692524 \cdot exp(-7)$	$1/min$
$k_{ELS,out}$	$1 \cdot exp(-3)$	$2.134605 \cdot exp(-3)$	$1/min$
k_{NU}	$1 \cdot exp(0)$	$1.353370 \cdot exp(-1)$	$1/min$
k_{UA}	$1 \cdot exp(0)$	$1.887060 \cdot exp(-2)$	$1/min$
k_{UD}	$1 \cdot exp(-3)$	$7.696937 \cdot exp(-7)$	$1/min$
$k_{cat,UN,ELS}$	$1 \cdot exp(+1)$	$7.317552 \cdot exp(-1)$	$1/min$
$K_{m,UN,ELS}$	$1 \cdot exp(-2)$	$8.811663 \cdot exp(-2)$	mg/L
$k_{cat,AU,KJE}$	$1 \cdot exp(+1)$	$1.770906 \cdot exp(-3)$	$1/min$
$K_{m,A,KJE}$	$1 \cdot exp(-2)$	$1.712596 \cdot exp(+1)$	mg/L
$K_{m,U,KJE}$	$1 \cdot exp(-2)$	$2.551816 \cdot exp(-4)$	mg/L